Zeeman spectroscopy of the vanadium luminescence in GaP and GaAs

G. Aszodi*
4. Physikalisches Institut der Universität Stuttgart, D-7000 Stuttgart 80, Pfaffenwaldring 57, West Germany

U. Kaufmann
Fraunhofer Institut für Angewandte Festkörperphysik, D-7800 Freiburg, Eckerstrasse 4, West Germany
(Received 16 April 1985; revised manuscript received 25 July 1985)

A high-resolution study of the vanadium-induced A and B luminescence zero-phonon lines in GaP:V and GaAs:V is presented. The Zeeman splitting of line A (and that of B in GaAs) in fields up to 5.3 T has been investigated in detail. The analysis of the data strongly indicates that earlier assignments of lines A and B to V^{2+} ($3d^3$) must be revised and that the A,B lines must be assigned to the ${}^3T_2 \rightarrow {}^3A_2$ crystal-field transition of $V^{3+}(3d^2)$. The A-B splittings in zero field can be well accounted for in terms of Ham's theory of the dynamic Jahn-Teller effect. The strength of the vibronic coupling is found to be moderate, $E_{JT}/\hbar\omega \approx 3.7$, thus suggesting that a Jahn-Teller–induced static distortion does not occur. The dynamic Jahn-Teller model also provides a satisfactory description for the Zeeman splittings of lines A and B. Some very fine spectral details (< 1 cm^{-1}), however, appear to be related to residual strains in the samples investigated.

I. INTRODUCTION

Vanadium doping of GaP, GaAs, and InP gives rise to a characteristic crystal-field luminescence band in the 1.5-μm–1.7-μm wavelength range. In each compound the band is dominated by a zero-phonon (ZP) line A and a second, "hot" ZP line B at energies of 10 cm^{-1} (GaAs), 15 cm^{-1} (GaP) (Ref. 1), and 12 cm^{-1} (InP) (Ref. 2) above the "cold" line A. In GaP and GaAs this luminescence had been attributed to a crystal-field transition of $V^{2+}(3d^3)$ (Refs. 1, 3, and 4) and preliminary Zeeman results for line A were thought to support this assignment.[1] On the other hand, recent Zeeman studies of lines A and B in InP (Refs. 2 and 5) revealed that the V luminescence in InP must be attributed to a crystal-field transition of $V^{3+}(3d^2)$, and this assignment was found to be consistent with the results of uniaxial stress studies.[6]

As first pointed out by Skolnick *et al.*[2] the similarity of the GaP:V and GaAs:V spectra with the InP:V luminescence spectrum suggests that the A and B ZP lines in GaP and GaAs arise from V^{3+} as well in contrast to the earlier V^{2+} assignments. Subsequent Zeeman[7] and stress studies[8] for GaAs:V supported this suggestion.

To resolve these contradicting interpretations, new Zeeman results for GaP:V and GaAs:V are reported in this work. On the basis of these data we come to the conclusion that the earlier V^{2+} assignment of the GaP:V and GaAs:V luminescence band must be revised and that these bands have to be assigned to the ${}^3T_2(F) \rightarrow {}^3A_2(F)$ crystal-field transition of $V^{3+}(3d^2)$.

II. EXPERIMENTAL PROCEDURE

Most of the experimental results to be reported here were obtained with the same GaP:V and GaAs:V samples used in the previous work of Kaufmann *et al.*[1] Some data were taken with other samples cut from the same GaP:V and GaAs:V slices. It was noticed that samples from one and the same slice did not exhibit identical shapes of the ZP lines A and B in zero magnetic field. The Zeeman spectra were taken with the same setup used previously[1] but with considerably improved spectral resolution (≤ 0.3 cm^{-1}). All spectra were taken in the Voigt configuration ($\mathbf{H} \perp \mathbf{k}$) using a superconducting split-coil magnet with a maximum magnetic field H_{max} of 5.3 T.

III. EXPERIMENTAL RESULTS AND ASSIGNMENTS

A. Shape of lines A and B in zero magnetic field

A high-resolution spectrum of lines A and B in the GaAs:V sample used for most Zeeman studies is shown in Fig. 1. Both lines exhibit a high-energy shoulder A^0 and B^0, 0.8 and 0.5 cm^{-1} above the main components A^x and

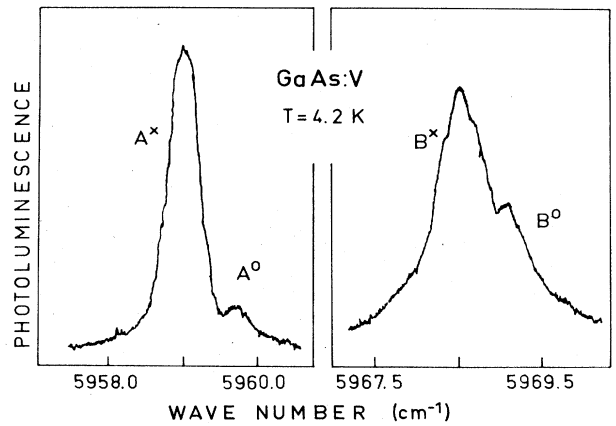

FIG. 1. Shape of the ZP lines A and B of GaAs:V in zero magnetic field.

B^x. The shoulder A^0 has not been observed in every sample investigated, thus suggesting that it is split off from the main line A^x by internal strains. The present B^x-B^0 splitting is a factor of 2.5 larger than that found in absorption measurements[9] and thus also appears to be strain enhanced. The relative intensities of lines A and B were measured in the temperature range 5—40 K. From an Arrhenius plot of the data the hot line B was found to lie 10.4 cm^{-1} above line A, in good agreement with the directly measured spectroscopy splitting of 9.6 cm^{-1}. This proves that the splitting between lines A and B arises exclusively from a splitting of the excited luminescence state and that transitions A and B have the same final state.

In GaP:V the zero-field shape of lines A and B (separation 15 cm^{-1}) is similar to that for GaAs:V. Line A consists of a main component A^x and a shoulder A^0, 1.0 cm^{-1} above A^x, while line B is split into two components with comparable intensity, separated by 1.0 cm^{-1},[1] too.

B. Zeeman splittings for GaAs:V

The development of the Zeeman splitting of line A for $\mathbf{H}||\langle 100\rangle$ is shown in the left part of Fig. 2 and the corresponding 5.3-T spectrum is traced in the left part of Fig. 3. These figures reveal details which were not evident in the preliminary lower-resolution data mentioned for GaAs:V in Ref. 1, namely, the splitting of line A is not symmetrical with respect to the zero-field position and some of the Zeeman components vary nonlinearly with applied field. The nonlinear components 1, 3, and 5 (crosses in Fig. 2) emerge from A^x while the linear components 2, 4, and 6 (circles) seem to emerge from the shoulder A^0. Thus, it is evident from Figs. 2 and 3 that line A splits into nine components under $\mathbf{H}||\langle 100\rangle$. This finding invalidates the previous[1] assignment where line A was assigned to a transition from a twofold to a fourfold degenerate state and indicates that the transition occurs between two threefold degenerate states. The stick diagram below the spectrum in Fig. 3 reflects the polarization properties of the Zeeman components. The magnetic-field splitting of line A in GaAs for $\mathbf{H}||\langle 111\rangle$ and $\mathbf{H}||\langle 110\rangle$ is plotted in Figs. 4(a) and 4(b).

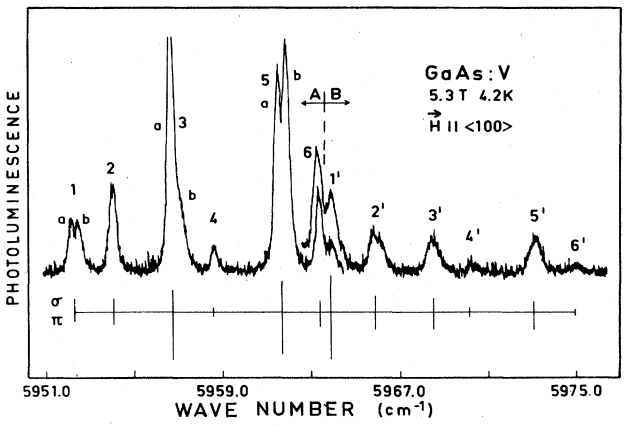

FIG. 3. Zeeman splittings of line A (left) and line B (right) in GaAs:V for $\mathbf{H}||\langle 100\rangle$ and $H=5.3$ T.

The full angular variation of the components 5a, 5b, and 6 upon rotation of the field in a (110) plane is displayed in Fig. 5. From Figs. 2—5 it is obvious that the positions of all nine Zeeman components emerging from line A are anisotropic. However, the splittings 2-4 and 4-6 are isotropic as are the 1-3 and 3-5 splittings. They correspond to g factors between 1.88 ± 0.04 and 1.94 ± 0.04. The latter value is obtained from the $\mathbf{H}||\langle 111\rangle$ spectrum and is considered to be the most accurate one. This g value is very close to the ground-state g factor of V^{3+} in GaAs, $g=1.957$, as determined by electron-spin resonance.[1]

Line B in GaAs:V splits into six Zeeman components for $\mathbf{H}$ along $\langle 100\rangle$, Figs. 2 and 3. The linear components are again shown as circles in Fig. 2. This subpattern is identical with the corresponding one of line A. The very

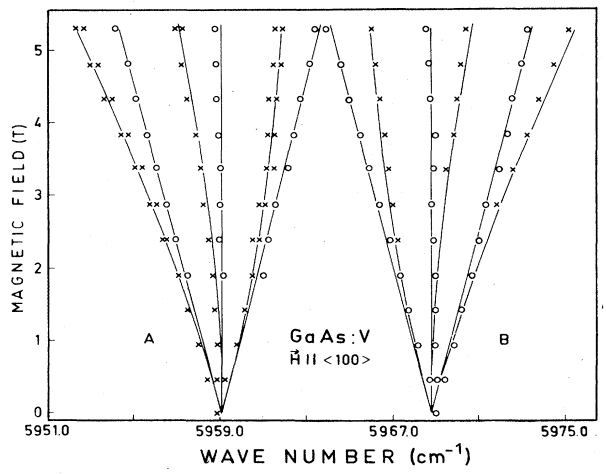

FIG. 2. Development of the Zeeman splitting of lines A and B in GaAs:V for $\mathbf{H}||\langle 100\rangle$. Circles and crosses denote lines which vary linearly and quadratic, respectively, with magnetic field. The curves are a fit based on Eqs. (4).

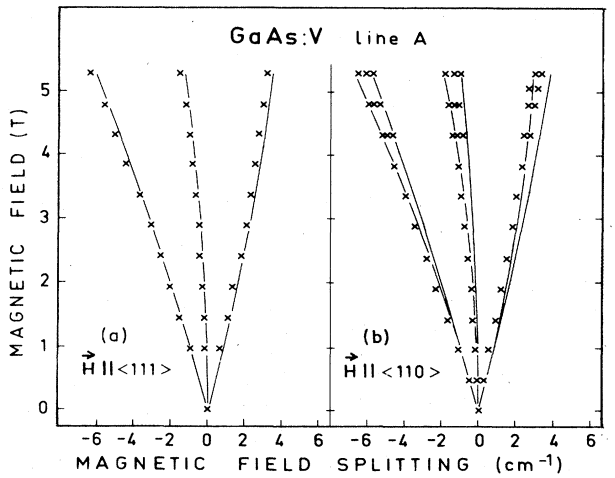

FIG. 4. Development of the Zeeman splitting of line A in GaAs:V for (a) $\mathbf{H}||\langle 111\rangle$ and (b) $\mathbf{H}||\langle 110\rangle$. The curves are a fit based on Eqs. (7a) and (7b).

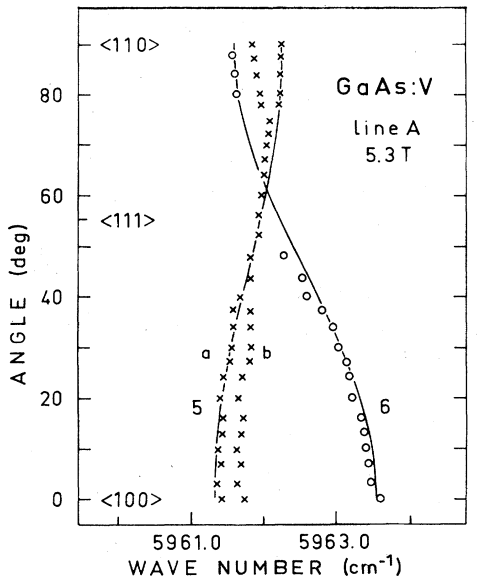

FIG. 5. Angular dependence of lines 5a, 5b, and 6 upon rotation of the magnetic field in a (110) plane.

small doublet splitting of the nonlinear components, seen for line A, has not been resolved for line B possibly because the components of B were recorded with lower resolution to improve the signal-to-noise ratio. When the magnetic field is along a $\langle 110 \rangle$ direction line B was found to split into 10 components (not shown here). Since we already noted that the final state in the transitions A and B is triply degenerate one must conclude that the initial state for transition B has a degeneracy greater than 3.

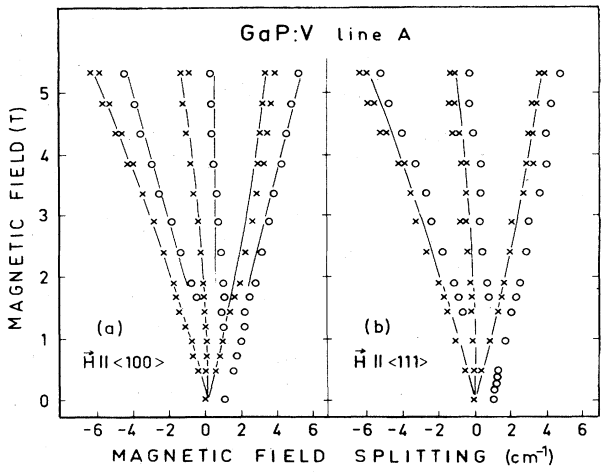

FIG. 6. Development of the Zeeman splitting of line A in GaP:V for (a) $\mathbf{H}||\langle 100 \rangle$ and (b) $\mathbf{H}||\langle 111 \rangle$. The Zeeman components which seem to emerge from A^0, cf. Fig. 3, are denoted by circles, those emerging from A^x are denoted by crosses. The full curves are a fit based on (a) Eqs. (4) and (b) Eqs. (7a) and 7(b); see the text.

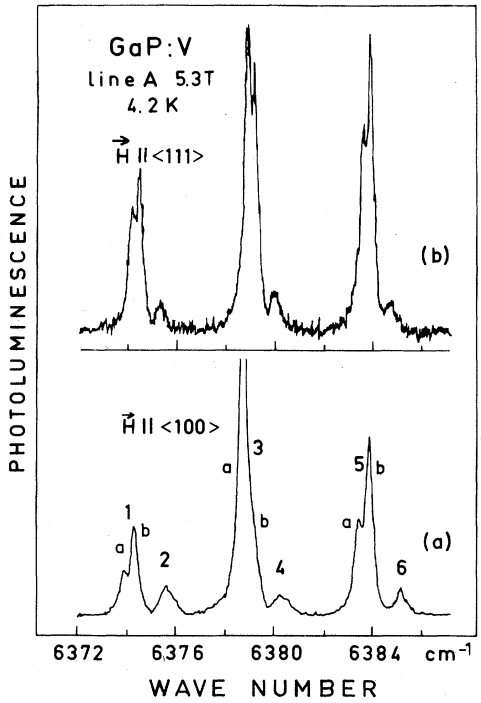

FIG. 7. Zeeman splitting of line A in GaP:V at 5.3 T for (a) $\mathbf{H}||\langle 100 \rangle$ and (b) $\mathbf{H}||\langle 111 \rangle$.

C. Zeeman splittings for GaP:V

In many respects the Zeeman splitting of line A in GaP:V is almost identical with that of line A in GaAs:V. This is especially obvious from a comparison of the GaP:V splittings for $\mathbf{H}||\langle 100 \rangle$ in Figs. 6(a) and 7(a) with the corresponding GaAs:V data in the left-hand side of Figs. 2 and 3. The thermalization behavior of the nine components in Fig. 7(a) was investigated by comparing spectra taken at sample temperatures of 5 and 2 K, respectively. The weaker components 2, 4, and 6 were found to thermalize into the doublets 1, 3, and 5. Thermalization, however, neither occurred between the components 2, 4, and 6 nor between 1, 3, and 5. This strongly suggests that the 2-4-6 as well as the 1-3-5 splitting directly reflects the magnetic-field splitting of the ground state, while the small splittings, e.g., 1a-1b-2, occur in the excited state. The g value evaluated from the large isotropic splittings is $g = 1.98 \pm 0.04$. The $\mathbf{H}||\langle 111 \rangle$ splitting of line A in GaP:V, Figs. 6(b) and 7(b), is qualitatively somewhat different from that in GaAs:V: No collapsing into three lines is observed, instead nine lines are still resolved. The angular dependence in Fig. 8 reveals that this is true over the full angular range. Contrary to GaAs:V the anisotropy of the line positions is very small, ≈ 0.7 cm^{-1} or less. As for GaAs:V the 1-3-5 and the 2-4-6 splittings are isotropic. Together with the thermalization behavior described before this indicates a triplet final state with an isotropic g value, $g \approx 2$.

IV. COMPARISON WITH THEORETICAL MODELS

Since the experimental data for GaP:V and GaAs:V presented here are very similar we will discuss both sys-

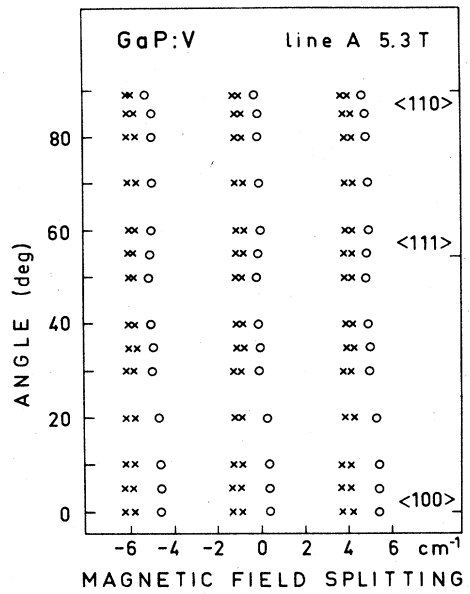

FIG. 8. Angular dependence of the Zeeman components of line A in GaP:V at 5.3 T. The magnetic field is rotated in a (110) plane.

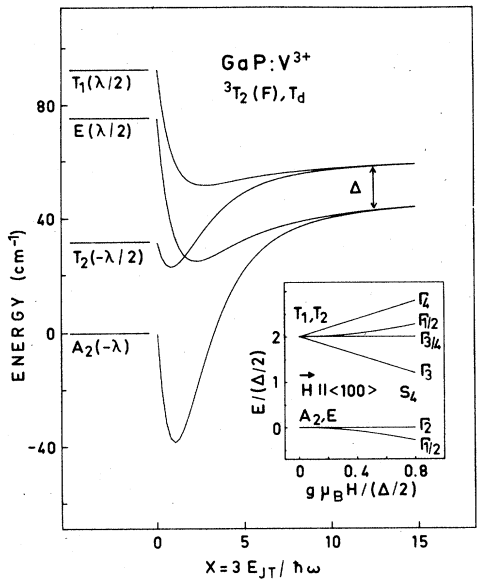

FIG. 9. Spin-orbit splitting of the $^3T_2(F)$ term of $V^{3+}(3d^2)$ as obtained from a numerical diagonalization of the complete static crystal-field matrices (left). With increasing JT coupling the four electronic levels merge into a threefold and a sixfold degenerate vibronic level with limiting splitting Δ, see Eqs. (2a)—(2d). Note that the energetic positions of the four spin-orbit levels in the present treatment are significant only for $x > 3$. Shown in the inset is the normalized Zeeman splitting of the two vibronic levels as calculated from Eqs. (4) in the limit $x \gg 1$.

tems together. In the preceding section we have already argued that transition A occurs between an excited triplet state and a triplet ground state, the latter having an isotropic g value, $g \lesssim 2$. This result is incompatible with previous $V^{2+}(3d^3)$ assignments of line A in GaP:V and GaAs:V and indicates that line A has to be attributed to $V^{3+}(3d^2)$ as suggested by Skolnick *et al.*[2] on the basis of similar results for InP:V. In the following, it will be demonstrated that this assignment is fully consistent with the predictions of crystal-field theory provided that electron-phonon interaction [Jahn-Teller (JT) effect] and effects due to random strains are properly accounted for.

A. Static crystal-field model

For the V^{3+} ion in tetrahedral symmetry (T_d) the lowest crystal-field terms $^3A_2(F)$, $^3T_2(F)$, $^3T_1(F)$, and $^1E(D)$,[10,11] arise from the free-ion LS terms ^3F and ^1D. The excited states $^3T_2(F)$ and $^3T_1(F)$ lie $10Dq$ and $18Dq$ above the $^3A_2(F)$ ground state where Dq is the cubic crystal-field parameter. The position of the $^1E(D)$ term depends on Dq and on the Racah parameters B and C, the latter two describing the interelectronic $3d$-electron Coulomb interaction. With spin-orbit interaction included, the ground state becomes a T_2 spin-orbit level while the $^3T_2(F)$ term splits into four spin-orbit levels A_2, T_2, E, T_1 as shown in the left part of Fig. 9.

The positions of the four spin-orbit levels were calculated by numerical matrix diagonalization of the complete $3d^2$ energy matrices[12] containing Coulomb (B,C), crystal-field (Dq), and spin-orbit (λ) interaction. The parameter Dq was first fixed by fitting the $^3T_2$ term to the center of gravity of the mirror image of the GaP:V and GaAs:V luminescence bands. This gives Dq values of 650 and 610 cm^{-1}, respectively. The ratio of B/C was taken as the free-ion value $B_0/C_0 = 4.8$.[13] Experience with other transition ions in III-V compounds suggests that the B parameter is reduced by about 50% from the free-ion value, $B_0 = 860$ cm^{-1} for V^{3+}.[13] In the present case B was chosen somewhat larger, 530 and 510 cm^{-1} for GaP and GaAs, respectively, such that the $^3T_2(F)$ spin-orbit splitting, see Fig. 9, no longer depends critically on this parameter. The numerical diagonalizations were then performed with a starting value for the spin-orbit-coupling constant λ of 70 cm^{-1} [free-ion value $\lambda_0 = 103$ cm^{-1} (Ref. 13)]. The final choice for λ, 65 and 51 cm^{-1} for GaP and GaAs, respectively, will be justified in the next section. The $^3T_2(F)$ splitting for GaP:V shown in the left part of Fig. 9 has been calculated with the GaP:V parameters quoted above.

According to the Zeeman data presented in Sec. III B, transition A must start from a threefold-degenerate (or nearly-degenerate) state while transition B must start from an at least fourfold-degenerate state higher in energy by 15 cm^{-1} (GaP) and 10 cm^{-1} (GaAs). These requirements are not met by the spin-orbit levels of $^3T_2(F)$ in a static crystal-field model for any physically reasonable choice of Dq, B, C, and λ compare the left part of Fig. 9. This simple model must therefore be rejected. It will be shown in the next section, that the A-B zero-field splittings as well as the magnetic-field splittings can be well understood when the effect of vibronic coupling (JT effect) within $^3T_2(F)$ is taken into account.

B. Dynamic Jahn-Teller effect model

1. Zero magnetic field

Since the uniaxial stress data for InP:V (Ref. 6) and GaAs:V (Ref. 8) indicates a predominant electron-phonon coupling of the $^3T_2$ term to tetragonal, E-type vibrational modes, we will restrict the following considerations to this type of vibronic coupling. This coupling has quite a different effect on the first- and second-order spin-orbit splittings of $^3T_2$, see Fig. 9. It is therefore convenient to describe the $^3T_2$ spin-orbit splitting, correct to second order, by the effective Hamiltonian[14,15]

$$\mathscr{H}^{(2)}_{\text{s.o.}}=\zeta\mathbf{L}\cdot\mathbf{S}+\mu(\mathbf{L}\cdot\mathbf{S})^2+\rho(L_x^2S_x^2+L_y^2S_y^2+L_z^2S_z^2)\ , \tag{1}$$

where the parameters ζ,μ,ρ in the present case were obtained by comparison with the exact numerical diagonalization of the d^2 crystal-field matrices. When the JT interaction is now included the relative energies of the four, vibronic ground state, $^3T_2$ spin-orbit levels as a function of ζ,μ,ρ and the strength of the JT coupling, measured by $x=3E_{\text{JT}}/\hbar\omega$, are then given by[16]

$$E(A_2)=-2\gamma(x)\zeta+2[1+\gamma(x)]\mu+2\rho+4K_1+2K_2\ , \tag{2a}$$

$$E(T_2)=-\gamma(x)\zeta+\mu+\rho+K_1+K_2\ , \tag{2b}$$

$$E(E)=\gamma(x)\zeta+[2-\gamma(x)]\mu+2\rho+K_1+2K_2\ , \tag{2c}$$

$$E(T_1)=\gamma(x)\zeta+\mu+\rho+K_1+K_2\ , \tag{2d}$$

where $\gamma(x)=\exp(-x/2)$ is the JT reduction factor appropriate for E-mode coupling,[17] E_{JT} is the JT stabilization energy of the vibronic ground state and $\hbar\omega$ is the energy of the effective E-mode coupling to $^3T_2$. It should be noted that Eqs. (2a)—(2d) are a good approximation only if the JT interaction is sufficiently large compared with the first-order spin-orbit interaction. In the present case, this requires $x>3$. The vibronic sidebands of the ZP line A suggest $\hbar\omega\simeq 90$ cm^{-1} for GaP and $\hbar\omega\approx 70$ cm^{-1} for GaAs. These values have been used in numerical calculations where $\hbar\omega$ enters explicitly. The expressions (2a)—(2d) also contain effects due to second-order spin-orbit coupling of the vibronic ground state with excited vibronic states. They are proportional to $\lambda^2/\hbar\omega$ and are described by $K_1(x)$ and $K_2(x)$. The analytical form of $K_1(x)$ and $K_2(x)$ is given in the original work of Ham.[17] The relative energies of the $^3T_2$ spin-orbit levels as calculated from Eqs. (2a)—(2d) are plotted versus the coupling strength x in Fig. 9. Superimposed on each level, but not included in this figure, is the JT stabilization energy E_{JT} which for $x\gg 1$ is given by $E_{\text{JT}}=x\hbar\omega/3$. With increasing coupling strength, the first-order spin-orbit splitting becomes quenched while the second-order splitting, E-T_1, remains almost unaffected. The limiting splitting Δ between the lower A_2, E triplet, and the higher-lying sextet T_1,T_2 is given by $\Delta=\mu+\rho+K_2$. These threefold and sixfold, quasidegenerate vibronic states have all the properties which the magnetic-field splittings indicate for the excited states of the ZP transitions A and B, see Secs. III B and III C. We therefore reassign the ZP lines A and B in GaP and in GaAs to transitions from these two states to the $T_2\,{}^3A_2$ ground state of V^{3+}. The limiting splitting Δ in Fig. 9 then corresponds to the spectroscopic splitting between lines A and B. To fit the A-B splittings requires a V^{3+} spin-orbit coupling constant λ of 65 cm^{-1} in GaP, see Fig. 9, and 51 cm^{-1} in GaAs. This corresponds to a covalency reduction of 37 and 50%, respectively. Especially the latter value is larger than usually assumed but still appears to be reasonable. For instance, with $\lambda=51$ cm^{-1} and $Dq=610$ cm^{-1} from Sec. IV A, the GaAs:V^{3+} ground-state g factor is predicted as $g=1.955$ in favorable agreement with the experimental value, $g=1.957$.[1]

With the above λ values the triplet-sextet splitting, compare Fig. 9, is close to the A-B splittings already for $x\geq 10$. On the other hand, to account for the very small zero-field splitting of line B in GaP:V (Ref. 1) and GaAs:V (Ref. 9) in terms of the residual T_1-T_2 splitting, x must be smaller than 12. Thus, we have $x\approx 11$ or $E_{\text{JT}}/\hbar\omega\approx 3.7$ for both GaP and GaAs which corresponds to a moderately strong dynamic JT interaction.

Transitions from the four spin-orbit levels in Fig. 9 to the $T_2\,{}^3A_2$ ground state of V^{3+} are electric dipole ($E1$) allowed with the exception of the $A_2\rightarrow T_2$ transition which is only magnetic dipole ($M1$) allowed. This transition, however, becomes weakly $E1$ allowed when A_2 is mixed by tetragonal strains with the nearby E level. This suggests that the shoulder A^0 in Fig. 1 arises from the A_2 level. According to Fig. 9, however, one would expect this shoulder on the low-energy side of the main component A^x. We suggest that this reversal also results from the action of residual internal strains. Other weak interactions like spin-spin coupling[18] are unlikely responsible for the A^0-A^x zero-field splitting since this splitting has not been observed in all samples investigated. On the basis of the $E1$ selection rules and the influence of strains we thus qualitatively understand why line A contains a strong and a weak component while line B consists of two components with comparable intensity in zero magnetic field, see Fig. 1 and Refs. 1 and 9.

2. Magnetic-field splittings

For $x=3E_{\text{JT}}/\hbar\omega\approx 11$ the orbital contribution to the Zeeman interaction within the $^3T_2$ term is almost completely quenched.[17] To a good approximation the linear Zeeman interaction within the $^3T_2$ vibronic ground state can then be described by the operator

$$\mathscr{H}^{(1)}_H=g\mu_B\mathbf{S}\cdot\mathbf{H}\ , \tag{3}$$

with g close to the free-spin value 2.002 (Ref. 19) and $S=1$. When $\mathbf{H}$ is along $\langle 100\rangle$ the eigenvalues of $\mathscr{H}^{(1)}_H$ (including the zero-field splitting Δ) are found to be given by

$$E(\Gamma_{3/4},\Gamma_2)=\Delta/2\pm\Delta/2\ , \tag{4a}$$

$$E(\Gamma_4,\Gamma_3)=\pm g\mu_BH+\Delta\ , \tag{4b}$$

$$E(\Gamma_{1/2},\Gamma_{1/2})=(\Delta/2)\{1\pm[1+(g\mu_BH)^2/(\Delta/2)^2]^{1/2}\}\ . \tag{4c}$$

These eigenvalues are plotted in the inset of Fig. 9 and it is seen that three of them retain a twofold accidental degeneracy. The A_2, E triplet shows only a quadratic Zeeman splitting where the linear component Γ_2 derives from A_2 and the degenerate "quadratic" Γ_1,Γ_2 components derive from the E level. It will be shown below that the accidental Γ_1,Γ_2 degeneracy is not lifted when $\mathbf{H}$ is rotated in a (110) plane. A comparison of the inset in Fig. 9 with Figs. 2 and 6(a) allows to explain the $\mathbf{H}||\langle 100\rangle$ splittings of lines A and B: The linear components in Figs. 2 and 6(a) derive from the linear levels $\Gamma_2(A_2)$ and $\Gamma_{3/4}$ (T_1,T_2) in Fig. 9. The nonlinear components derive from the two quadratic levels in the inset of Fig. 9. The fit in Figs. 2 and 6(a) is based on Eqs. (4a), 4(b), and 4(c) with $g=2$ for the $^3T_2$ state and $g=1.96$ for the $T_2\,{}^3A_2$ ground state. The latter g value corresponds to that determined for GaAs:V^{3+} by electron-spin resonance.[1]

When $\mathbf{H}$ is not parallel to $\langle 100\rangle$ the Hamiltonian in Eq. (3) no longer can be solved analytically. However, as long as $g\mu_B H \ll \Delta$, we can simulate its effect within the vibronic A_2,E triplet by the effective Hamiltonian

$$\mathscr{H}_H^{(2)} = q \sum_{x,y,z} S_i^2 H_i^2 , \tag{5}$$

where q is a constant which, correct to second-order perturbation theory within the $^3T_2$ vibronic ground state, is given by

$$q = -(g\mu_B)^2/\Delta . \tag{6}$$

The eigenvalues of $\mathscr{H}_H^{(2)}$ upon rotation of $\mathbf{H}$ in a (110) plane are found to be given by

$$E(E1)=E(E2)=qH^2(1-\tfrac{1}{2}\sin^2\theta) , \tag{7a}$$

$$E(A_2)=qH^2\sin^2\theta , \tag{7b}$$

where θ is the angle between $\mathbf{H}$ and the $\langle 001\rangle$ direction. The degeneracy between $E(E1)$ and $E(E2)$ is lifted when $H_x \neq H_y$ but also by tetragonal strains.

Equations (7a) and (7b) with the appropriate angles were used to fit the $\mathbf{H}||\langle 111\rangle$ and $\mathbf{H}||\langle 110\rangle$ Zeeman splittings of line A in GaAs:V, Fig. 4 and in GaP:V, Fig. 6(b). The full curves in these figures were drawn with $g=2$ for the $^3T_2$ state and with $g=1.96$ for the $T_2\,{}^3A_2$ ground state. In the case of GaAs:V^{3+}, the condition $g\mu_B H_{\max} \ll \Delta$ is not satisfied. Therefore $qH^2_{\max}=1.9$ cm^{-1} was used instead of the second-order result, Eq.(6), which predicts $qH^2_{\max}=2.5$ cm^{-1}. For GaP:V^{3+}, on the other hand, the second-order result, $qH^2_{\max}=1.6$ cm^{-1} has been used. Except for the very small splittings (≈ 0.3 cm^{-1}) the data in Figs. 4(a), 4(b), and the dominant doublet lines in Fig. 6(b) are well reproduced.

On the basis of Eqs. (7a) and (7b) one can also account for the angular dependence of the GaAs:V^{3+} Zeeman components 5a, 5b, and 6 in Fig. 5. The curves in this figure were plotted with $qH^2_{\max}=1.9$ cm^{-1} as before. However, to fit the data we found it necessary to introduce a zero-field splitting, $\delta=0.3$ cm^{-1}, between $E(A_2)$ and $E(E)$ in Eqs. (7a) and (7b). This explains why the curves cross near 60° and not at 55° ($\mathbf{H}||\langle 111\rangle$).

The GaP:V angular dependence in Fig. 8 has a cubic shape since the singlet and doublet components never cross and since a third extremum occurs for $\mathbf{H}||\langle 111\rangle$. This cannot be explained by the formulas in Eqs. (7a) and (7b). The singlet amplitudes in Fig. 8 are ≈ 0.7 cm^{-1} while the residual singlet-doublet splittings at $\mathbf{H}||\langle 111\rangle$ are ≈ 1.0 cm^{-1} which is equal to the zero-field splitting of line A.[1] Since we suspect that the major contribution to the latter splitting arises from strains, we have the situation that strain effects are of the same order of magnitude as the Zeeman anisotropy. In such a case Eqs. (7a) and (7b) are no longer valid and the strain and Zeeman interaction within A_2,E has to be treated on an equal footing. This is beyond the scope of the present work.

We finally want to discuss the doublet splittings (≈ 0.3 cm^{-1}) of the nonlinear Zeeman components in Figs. 2, 3, 4(b), and 5 for GaAs:V and in Figs. 6, 7, and 8 for GaP:V. It has already been pointed out that such a splitting arises when H_x is not exactly equal to H_y since $E(E1)$ and $E(E2)$ in Eq. (7a) are then no longer degenerate. Therefore this splitting could arise from a slight misorientation of the sample. However, this possibility is considered quite unlikely since the samples were carefully oriented and since the splittings did not vary after repeated mountings of the samples. We therefore suggest that these fine splittings are induced by tetragonal strains which split the E level in Fig. 9 already in zero field.

3. *Polarization and thermalization behavior for* $\mathbf{H}||\langle 100\rangle$

The polarization properties of the Zeeman components have been studied in detail for the special case where $\mathbf{H}$ is

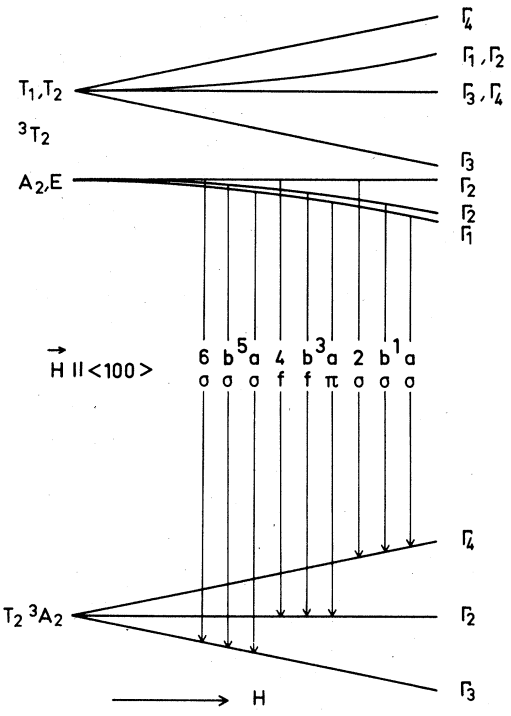

FIG. 10. Schematic magnetic-field splitting of the $V^{3+}\,{}^3A_2$ ground state and $^3T_2$ excited state for $\mathbf{H}||\langle 100\rangle$ and $x \gg 1$. The transitions giving rise to the nine Zeeman components of line A are shown together with the $E1$ polarization selection rules.

TABLE I. Intensity of the $\mathbf{H}||\langle 100\rangle$ Zeeman components of line A in GaP:V^{3+} for σ and π polarization.

No.	1a	1b	2	3a	3b	4	5a	5b	6
π	33	48	18	1000	~230	25	104	133	12
σ	198	372	138	146	84	85	349	646	107
σ/π	6.0	7.8	7.7	0.15	0.37	3.4	3.4	4.9	8.9
Theory	σ	σ	σ	π	f	f	σ	σ	σ

along a $\langle 100\rangle$ axis, see Fig. 3 for GaAs:V and Table I for GaP:V. Shown in Fig. 10 is the level scheme for the ground and excited states of V^{3+} for $\mathbf{H}||\langle 100\rangle$ together with the transitions giving rise to the Zeeman components of line A in Figs. 3 and 7(a). The $E1$ polarization selection rules of these transitions in S_4 symmetry are also given in the figure. For GaAs the $E1$ polarization selection rules are not well obeyed presumably as a result of strain mixing of the states and/or partial $M1$ character of the transitions. Two features, however, still agree fairly well with the predicted $E1$ selection rules. This is the dominant π character of line 3a and the weakness of the $E1$ forbidden line 4. A comparison of Table I with Fig. 10 shows, that in the case of GaP the selection rules are well obeyed except for the "forbidden" lines 3b and 4.

We finally note that the thermalization behavior of the lines in Fig. 7(a), see Sec. III C, finds a simple explanation in the level scheme of Fig. 10.

V. CONCLUSION

We have shown that the A,B ZP structure of GaP:V^{3+} and GaAs:V^{3+} in zero field as well as the A,B magnetic-field splittings can be reasonably well accounted for in terms of Ham's theory[17] of the dynamic JT effect. To match the V^{3+} vibronic spin-orbit levels of the $^3T_2$ term with the A,B ZP structure requires $E_{JT}/\hbar\omega \approx 3.7$ for both GaP and GaAs and this is the only essential free-fitting parameter. Using E mode energies as indicated by the vibronic sidebands, see Sec. IV B 1, gives JT stabilization energies E_{JT} of $\simeq 330$ cm^{-1} for GaP and $\simeq 260$ cm^{-1} for GaAs. Together with $E_{JT}/\hbar\omega \approx 3.7$ this indicates a moderate vibronic coupling which unlikely is sufficiently strong to induce a static tetragonal distortion.

The experimental data for the corresponding V^{3+} luminescence in InP:V have been considered as evidence for a static JT distortion where the apparent reduced (tetragonal) symmetry is induced by strong vibronic coupling with E modes.[2,5,6] However, as judged from the very close similarity of the V^{3+} band in InP, GaAs, and GaP, the coupling strength in InP is quite unlikely much larger than found here for GaP and GaAs. Therefore the dynamic JT model is probably more appropriate for InP:V^{3+}, too. It should be noted, that the apparent tetragonal angular variation of the states from the A,E triplet, compare Fig. 9, upon rotation of the magnetic field in a (100) plane, see Fig. 11 of Ref. 5 does not necessarily imply a static JT distortion. The same type of angular dependence is predicted in the dynamic description used here. From Eq. (5) we find that

$$W_1 = qH^2 , \tag{8a}$$

$$W_{2/3} = \tfrac{1}{2} qH^2(1 \pm \cos 2\phi) \tag{8b}$$

for the angular variation of A_2,E where ϕ is the angle between $\mathbf{H}$ and a $\langle 100\rangle$ direction in the (001) plane.

Not only does the dynamic description appear to be more appropriate as far as the value of $E_{JT}/\hbar\omega$ is concerned, it also gives a better insight into the vibronic problem. First of all, one can determine the coupling strength and the JT energy which remain unspecified otherwise. Second, particular details of the spectra, e.g., the thermalization and polarization behavior of the lines become more transparent. Of course, the static JT description becomes equivalent with the dynamic one when allowance for tunneling between the static distortions is made.[6] However, in doing so, the JT distortion is no longer really static.

Crystal-field transitions of transition-metal impurities in III-V compounds are usually associated with the divalent ionic charge state of the metal. Vanadium is an exception to this rule. So far the only other trivalent luminescent ion is the isoelectronic $4d$ transition metal niobium. Although the Nb luminescence in GaP and GaAs originally has been tentatively attributed to Nb^{2+} (Ref. 20) Zeeman studies have clearly shown that the luminescent charge state is Nb^{3+}.[21,22]

It has been previously suggested that vandium introduces a near midgap acceptor level V^{3+}/V^{2+} in GaAs.[1,4,23] More recent work, however, casts doubts on this suggestion.[24] Thus further work to understand the semi-insulating properties of GaAs:V is required.

ACKNOWLEDGMENTS

One of the authors (G.A.) is grateful to M. Pilkuhn and his co-workers for their hospitality during his stay in Stuttgart and to the Deutscher Akadamischer Austauschdienst for financial support. We also thank G. Rupp, K. Thonke, and J. Windscheif for their help with several computer programs and for discussions, and B. Clerjaud and P. Koidl for very useful comments on the manuscript. The work of one of the authors (U.K.) was supported by the Bundesministerium für Forschung und Technologie of the Federal Republic of Germany.

*Permanent address: Research Institute for Technical Physics of the Hungarian Academy of Sciences, Budapest, Hungary.

[1]U. Kaufmann, H. Ennen, J. Schneider, R. Wörner, J. Weber, and F. Köhl, Phys. Rev. B **25**, 5598 (1982).

[2]M. S. Skolnick, P. J. Dean, M. J. Kane, Ch. Uihlein, D. J. Robbins, W. Hayes, B. Cockayne, and W. R. Mac Ewan, J. Phys. C **16**, L767 (1983).

[3]V. S. Vavilov, V. V. Ushakov, and A. A. Gippius, Physica **117B**, 191 (1983).

[4]A. V. Vasilev, G. K. Ippolitova, E. M. Omelianovski, and A. I. Ryskin, Fiz. Tekh. Poluprovodn. **10**, 571 (1976) [Sov. Phys. Semicond. **10**, 341 (1976)].

[5]M. J. Kane, M. S. Skolnick, P. J. Dean, W. Hayes, B. Cockayne, and W. R. Mac Ewan, J. Phys. C **17**, 6455 (1984).

[6]K. J. Nash, M. S. Skolnick, B. Cockayne, and W. R. Mac Ewan, J. Phys. C **17**, 6199 (1984).

[7]G. Armelles, J. Barrau, D. Thebault, and M. Brousseau, J. Phys. (Paris) **45**, 1795 (1984).

[8]G. Armelles, J. Barrau, and D. Thebault, J. Phys. C **17**, 6883 (1984).

[9]B. Clerjaud, C. Naud, C. Benjeddou, G. Guillot, P. Leyral, B. Devaud, and B. Lambert, *Proceedings of the 3rd International Conference Semi-Insulating III-V Compounds, Kah-Nee-Ta, 1984* (Shiva, Nantwich, 1984), p. 484.

[10]We use the Mulliken notation to denote states transforming as the irreducible representations of the tetrahedral group T_d. States in lower symmetry are denoted according to Koster *et al.*, see Ref. 11.

[11]G. F. Koster, J. O. Dimmock, R. G. Wheeler, and H. Statz, *Properties of the Thirty-two Point Groups* (MIT, Cambridge, Mass., 1963).

[12]A. D. Liehr and C. J. Ballhausen, Ann. Phys. (N.Y.) **6**, 134 (1959).

[13]B. N. Figgis, *Introduction to Ligand Fields* (Wiley, New York, 1966).

[14]J. Kanamori, Prog. Theor. Phys. **17**, 177 (1957).

[15]M. D. Sturge, Phys. Rev. B **1**, 1005 (1970).

[16]U. Kaufmann, P. Koidl, and O. F. Schirmer, J. Phys. C **6**, 310 (1973).

[17]F. S. Ham, Phys. Rev. **138**, A1727 (1965).

[18]P. Koidl, Phys. Status Solidi B **74**, 477 (1976).

[19]A slight deviation of the excited-state g factor from the spin-only value may result from admixture of other states through spin-orbit coupling. It is of the order of the ground-state g shift and therefore its neglect does not significantly affect any fit based on Eq. (3).

[20]V. V. Ushakov, A. A. Gippius, V. A. Dravin, and S. F. Kantser, Fiz. Tekh. Poluprovdn. **15**, 890 (1981) [Sov. Phys. Semicond. **15**, 890 (1981)].

[21]H. Ennen, G. Aszodi, J. Weber, U. Kaufmann, and A. Axmann, Ger. Phys. Soc. **18**, 672 (1983).

[22]G. Aszodi, H. Ennen, J. Weber, U. Kaufmann, and A. Axmann, Fourth "Lund" International Conference on Deep Level Impurities in Semiconductors, Eger, Hungary, 1983 (unpublished).

[23]H. Terao, H. Sunakawa, K. Ohata, and H. Watanabe, in *Semi-Insulating III-V Materials, Evian, 1982* (Shiva, Nantwich, 1982), p. 54.

[24]B. Clerjaud, J. Phys. C **18**, 3615 (1985).